ESA Contract 11407/NL/MV/CCN-3, COO-3

ESA RADIATION REPORT
ESA_QCA0018801T_C

TITLE
Impact of Test Conditions on TID Results for Commercial FPGA

EUROPEAN SPACE AGENCY
CONTRACT REPORT

The work described in this report was done under ESA contract. Responsibility for the contents resides in the author or organisation that prepared it.

	Name	Function	Date	Signature
Prepared :	Fredrik Sturesson - Saab Ericsson Space Mikael Wiktorson - Saab Ericsson Space			
Checked :				
Authorised :	Stanley Mattsson - Saab Ericsson Space Reno Harboe-Sørensen - ESA/ESTEC	TOS-QCA, Technical Officer		

Distribution
Complete :
Summary :

SUMMARY

The impact of static versus dynamic operation during Total Ionising Dose (TID) testing of commercially manufactured Field Programmable Gate Array (FPGA) has been verified using the Actel RT54SX16 as test vehicle. The samples, manufactured by Matsushita (MEC), were biased at 3.3V and irradiated using a Cobalt-60 source at a dose rate of 800 Rad(Si)/hour. With the device operating at 40MHz the measured total dose tolerance was increased significantly compared to low frequency or static testing.

The impact on total dose behaviour for protons was tested using an identical set-up as for Cobalt-60. Proton energy of 100 MeV with an equivalent dose rate of 7-10 kRad(Si)/hour. The proton results indicate very similar behaviour as for Cobalt-60. The 10 times higher dose rate in the proton test gave, however, rise to increased leakage current compared to the Cobalt-60 case.

DOCUMENT CHANGE RECORD

Changes between issues are marked with a left-bar.

Issue	Date	Paragraphs affected	Change information
1	1 Dec 2000	All	New document

TABLE OF CONTENTS   **PAGE**

1.   ABSTRACT

The impact of static versus dynamic operation during Total Ionising Dose (TID) testing of commercially manufactured Field Programmable Gate Array (FPGA) has been verified using the Actel RT54SX16 as test vehicle. The samples, manufactured by Matsushita (MEC), were biased at 3.3V and irradiated using a Cobalt-60 source at a dose rate of 800 Rad(Si)/hour. With the device operating at 40MHz the measured total dose tolerance was increased significantly compared to low frequency or static testing.

The impact on total dose behaviour for protons was tested using an identical set-up as for Cobalt-60. Proton energy of 100 MeV with an equivalent dose rate of 7-10 kRad(Si)/hour. The proton results indicate very similar behaviour as for Cobalt-60. The 10 times higher dose rate in the proton test gave, however, rise to increased leakage current compared to the Cobalt-60 case.

2.   INTRODUCTION

The time dependent growth and annealing of irradiation induced defects in VLSI circuits are very complex and highly dependent upon oxide processing. For non-hardened commercial processes the radiation response in practical dose rate regimes are generally dominated by field-oxide parasitic leakage, which normally exhibit a rapid recovery with annealing time and temperature. In a very low-dose rate environment the irradiation response will likely be controlled by the gate-oxide leakage.
For FPGA, the most application like test mode would probably be 100% dynamic test at high clock frequency. Traditionally total dose testing is performed at static condition. In order to characterise the irradiation response of commercially manufactured FPGA and the influence of the operation condition, the Actel RT54SX16 has been used as a test vehicle. Two samples per test conditions have been irradiated to a cumulated dose of 90 kRad(Si) with the five operation modes given in Table I. The elevated temperature has been chosen to give the same chip temperature as devices operated at high frequency. The frequency in the low frequency test is low enough not to generate any heat in the chip.

TABLE I
OPERATING CONDITIONS DURING IRRADIATION

TID Condition	Ambient Temperature	Operation Mode
Static / RT	Room Temperature	Static
Low Freq. / RT	Room Temperature	300 kHz Dynamic
Static / 55°C	55°C	Static
Low Freq. / 55°C	55°C	300 kHz Dynamic
High Freq.	Room Temperature[a]	40 MHz Dynamic

[a]When the device is operated at 40MHz the chip temperature is about 55°C.

In-situ measurements of function and standby current were performed. Pre, intermediate and post electrical measurements of the input/output voltage and leakage currents, propagation delay measurements on binning circuits were also performed.
Three total dose tests with protons have been performed for comparison of results between Cobolt-60 and proton total dose.

3.   EXPERIMENTAL

3.1   Test Vehicle

As test vehicle the Actel's RT54SX16 was used. It is the smallest FPGA in the new SX-family, with 16,000 logic gates. The die is of revision 1, manufactured in a 0,6μm-process. All tests have been performed on devices from the same lot. The date code was 0019.

Marking / *Top side*	Marking / *Bottom side*
Actel Logo	T6HP12
RT54SX16	001
CQ256C 0019	USA

The test vehicle has been programmed using about 95 % of available gates. The design is mainly filled with rings of a 64 bits long shift registers. Two different types of rings have been used, one only using the register cells and one using two combinatorial cells building one shift register.
For time measurement, a binning circuit was implemented in a small part of the device. One input was connected to a chain of 50 invert buffers that ended in an output of the device.

3.2   Test Methods

Dynamic operation mode total dose tests have been performed by loading toggled data into the device. The devices are tested for function using a "virtual golden chip" test method. The principal of the technique is to compare each output from the device with the correct data stored and controlled by a monitor board. To test for start-up problems, the bias to the devices was always turned off/on before function test. The supply current and case temperature of the devices were monitored continuously.
Pre-, intermediate- and post-irradiation electrical measurements have been performed on the parameters listed in Table II. The measurements were performed with SE's component tester, SZ M3000.

TABLE II
ELECTRICAL PARAMETERS AND CONDITIONS

Parameter	Conditions	Low Limit	High Limit
Standby Current ($I_{CCI} + I_{CCA}$)	Inputs = GND or V_{CCI} $V_{CCI} = 3.3V+10\%$ $V_{CCA} = 3.3V+10\%$ $V_{CCR} = 5.0V+5\%$	-	4 mA
Function Test	$V_{IL} = 0.8V$, $V_{IH} = 2.0V$ Test Frequency = 1 MHz $V_{CCI} = 3.3V-10\%$ $V_{CCA} = 3.3V-10\%$ $V_{CCR} = 5.0V-5\%$		
I_{IL}	$V_{IN} = GND$ $V_{CCI} = 3.3V+10\%$ $V_{CCA} = 3.3V+10\%$ $V_{CCR} = 5.0V+5\%$	$-10\mu A$	$10\mu A$
I_{IH}	$V_{IN} = V_{CCI}$ $V_{CCI} = 3.3V+10\%$ $V_{CCA} = 3.3V+10\%$ $V_{CCR} = 5.0V+5\%$	$-10\mu A$	$10\mu A$
V_{OL}	$I_{OL} = 12mA$ (TTL) $V_{CCI} = 3.3V+10\%$ $V_{CCA} = 3.3V+10\%$ $V_{CCR} = 5.0V+5\%$	-	0.5V
V_{OH}	$I_{OH} = - 8mA$ (TTL) $V_{CCI} = 3.3V-10\%$ $V_{CCA} = 3.3V-10\%$ $V_{CCR} = 5.0V-5\%$	2.4V	V_{CCI}
I_{OZL}	$V_{IN} = GND$ Output disabled $V_{CCI} = 3.3V+10\%$ $V_{CCA} = 3.3V+10\%$ $V_{CCR} = 5.0V+5\%$	$-10\mu A$	$10\mu A$
I_{OZH}	$V_{IN} = V_{CCI}$ Output disabled $V_{CCI} = 3.3V+10\%$ $V_{CCA} = 3.3V+10\%$ $V_{CCR} = 5.0V+5\%$	$-10\mu A$	$10\mu A$
Propagation Delays	$V_{CCI} = 3.3V-10\%$ $V_{CCA} = 3.3V-10\%$ $V_{CCR} = 5.0V-5\%$		

The used component tester is only able to treat one supply voltage to the tested device. V_{CCR} was instead supplied with an external power and set to 5,0V.

3.2.1   Propagation Delay Measurements

One small part of the device has been designed for parameter testing of propagation delays. Four binning circuits, two using buffer cells and two inverter cells were connected from inputs to outputs of the device. Each binning circuit consist of 50 cells. During irradiation the binning circuits were toggled with half the test frequency of the total dose test mode.

Positive and negative propagation delays were measured from input to output of these binning circuits. The component tester, SZ M3000, has a resolution of ±1 ns.

3.3   Conditions for I/Os During Irradiation

One small part of the device has been designed for parameter testing of I/Os. 40 of 208 available user I/Os were used for this purpose, some as inputs and some as outputs.

3.3.1   Inputs

User I/Os had three different states during irradiation,
- directly connected to Vcc=5V
- directly connected to GND
- toggled

The toggled inputs were driven by ACT logic (5V TTL, 5 fanouts logic with half the TID test frequency).
Dedicated inputs were controlled during irradiation. CLKA were toggled, CLKB driven high and FCLK hardwired to GND.

3.3.2   Outputs

Tristated I/Os during irradiation had three different external states
- outputs hardwired to Vcc=5V
- outputs hardwired to GND
- outputs left floating

Non-tristated I/Os had three different states during irradiation,
- static high with maximal load to GND
- static low with maximal load to Vcc=5V
- toggled with RC-load to GND

The toggled outputs had the same frequency as the toggled user inputs.

3.4 ^{60}Co-Facility

The total dose tests were performed at the hospital of Sahlgrenska. This hospital has a Cobalt-60 source suitable for low dose rate testing.
High temperature tests were performed by placing the devices in an oven and irradiating the oven and the test samples at the same time.
Staff from the Department of Radiofysik at Sahlgrenska hospital took care of dosimetry and beam calibration.

3.5   Proton Total Dose Tests

In total 6 samples were proton total dose tested at the Proton Irradiation Facility (PIF) at the Paul Scherrer Institute in Switzerland. All tests were carried out at room temperature to irradiation levels as also reached by ^{60}Co-test. Two samples were irradiated in static mode, two in dynamic at 300 kHz and two in dynamic at ~20MHz, The proton energy was 100MeV and the dose rate between 7 and 10 kRad(Si)/hour. Supply current and case temperature was measured during irradiation, but no timing or parameter measurements have been performed.

4.   RESULTS

4.1   Standby Current During ^{60}Co-Irradiation

The maximum limit for the standby current according to data specification is 4 mA. From Fig. 1, it could be seen that the supply current passed the limit around 50 kRad(Si) for static- and 300 kHz dynamic mode, while the 40 MHz mode was within specification limits to about 70kRad(Si). When the static and 300 kHz mode were repeated at elevated temperature (50°C), some annealing could be observed but it was not comparable to the effects at high frequency. By operating the FPGA in dynamic mode at 40 MHz and considering the leakage current, the total dose tolerance increased with a factor of 1,5. In earlier studies of Actel A1425A, this effect was even more pronounced [1].

Fig. 1 also shows the case temperatures monitored. The 300 kHz dynamic mode testing indicate no increased temperature. The 40 MHz dynamic mode testing causes the case temperature to increase to about 48°C. By measuring the temperature with a thermistor directly on the chip on a reference part, we have measured the chip temperature to be 50±2°C in the 40 MHz dynamic mode.

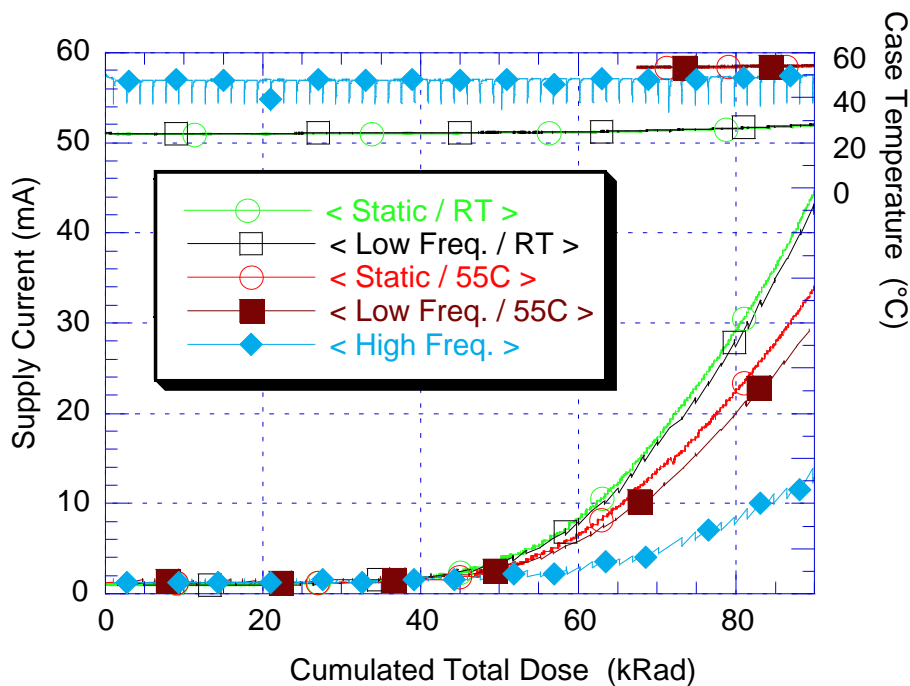No functional errors were detected in any of the total dose tests performed.

Fig. 1. Supply current as a function of total dose for the different test conditions. The upper part of the figure shows the case temperature for the three test conditions. The "dips" in the temperature curves for 40MHz dynamic test shows the decrease of case temperature in connection with the measurement of the static supply current lasting for about 3 minutes. The static and the 300 kHz curves follow each other very closely, both at room temperature and at elevated temperature. The annealing effect of frequency is clearly seen in the 40 MHz test, where the case temperature was about the same as the tests at elevated temperature.

4.2   I/O Damages from ^{60}Co-Irradiation

We have observed leakage current damages in all ^{60}Co tests performed. The input low and output low leakage currents (I_{IL}, I_{OZL}) are less pronounced and stay within specification limit (Fig. 2 and 7), while the results for the input high and output high leakage currents (I_{IH}, I_{OZH} in Fig. 3-6) are worse.

The state of the I/O during irradiation has a large impact of the results for the leakage currents. In Fig. 4 it can be seen that only inputs with a static high state are effected by irradiation. Only the static states on outputs indicate any deviation as shown in Fig. 6. The impact of different test conditions on some of the I/Os could be seen in Fig. 3 and 5 on selected type of inputs and outputs. Fig.7 show an example of a parameter where no impact from the different test conditions can be observed.

Similar tests of the I/Os at the A1425A [1] showed that the outputs decreased there drive capability with total dose. In Fig.8 showing the measurements of all high and low output voltages from all total dose test, it could be seen that RT54SX16 doesn't have this failure mode.
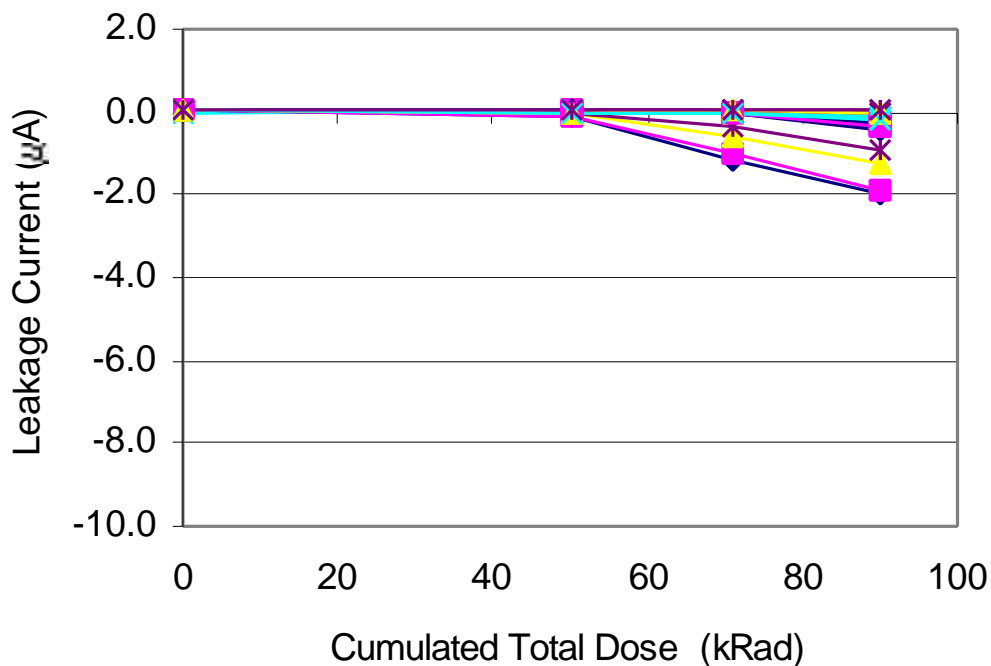

Fig. 2. Parameter measurements of Input Current Low (Iil) of all inputs for all five test conditions. The specification limit is ±10 µA. All data is mean values of each type of state of the inputs during irradiation.
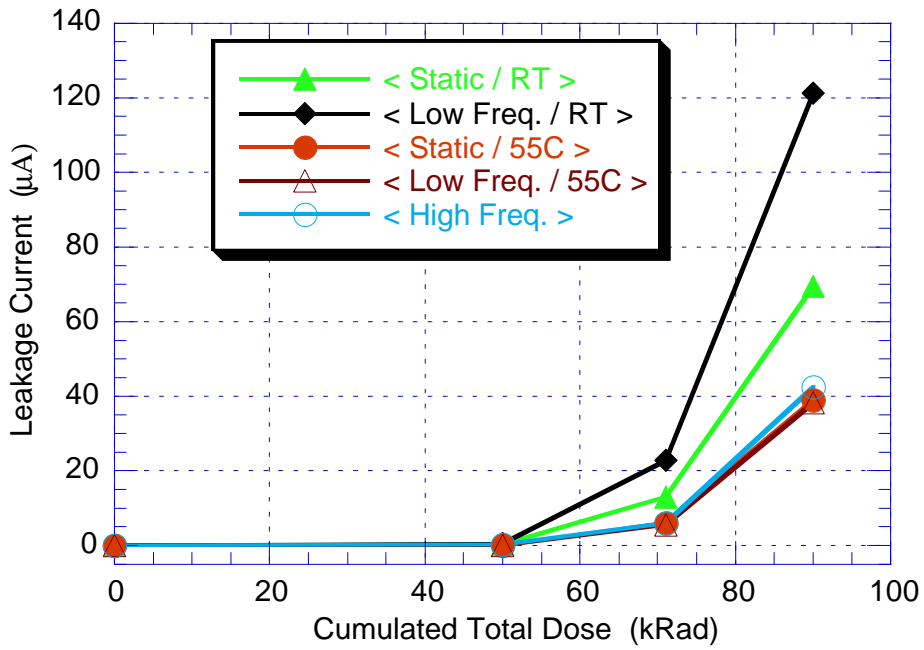
Fig. 3. Parameter measurements of Input Current High (I_{IH}) for the five test conditions. The specification limit is ±10 µA. Data show inputs that have been static high during irradiation, which was the worse case of all states.
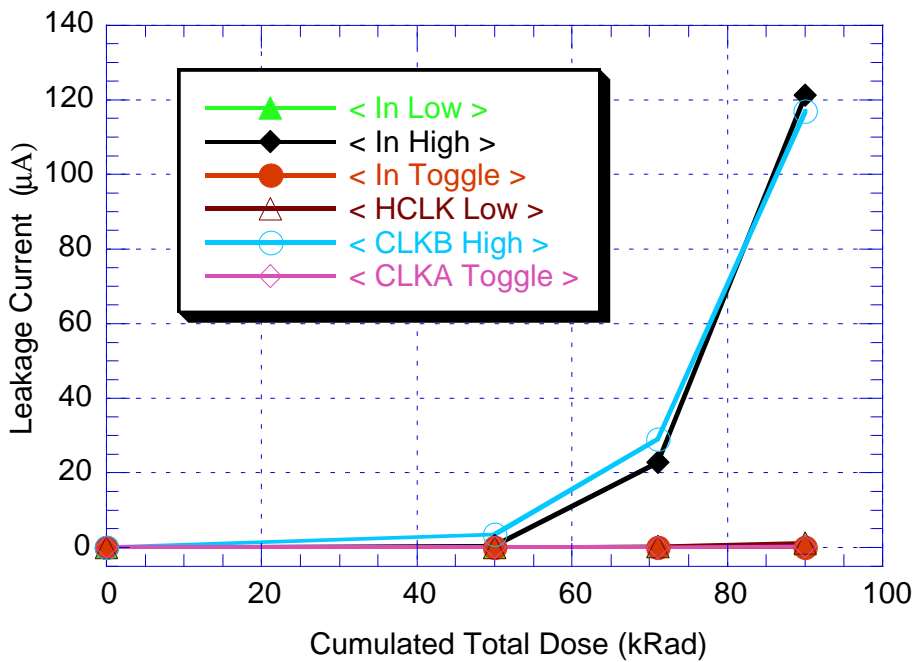

Fig. 4. Parameter measurements of Input Current High (I_{IH}) for the 300 kHz dynamic operation mode at room temperature. The specification limit is ±10 µA. Data show both user inputs and the dedicated clock inputs that have been static high, static low and toggled during irradiation. Input with static high and CKLB High showed worst degradation.
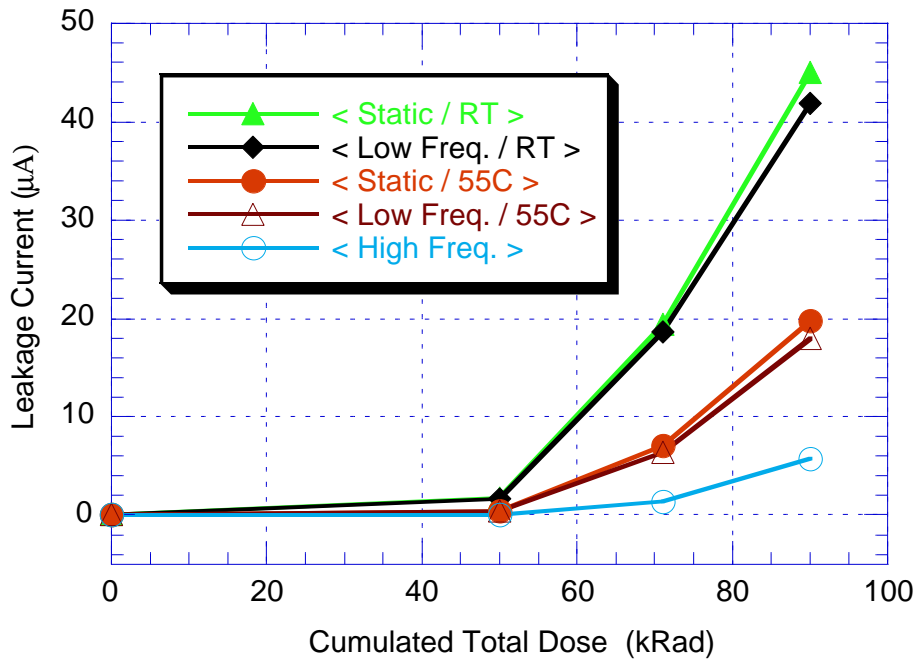
Fig. 5. Parameter measurements of Output Current High (I_{OZH}) for the five test conditions. The specification limit is ±10 µA. Data show outputs that have been static low during irradiation. Degradations follow very much the same pattern as the standby current.
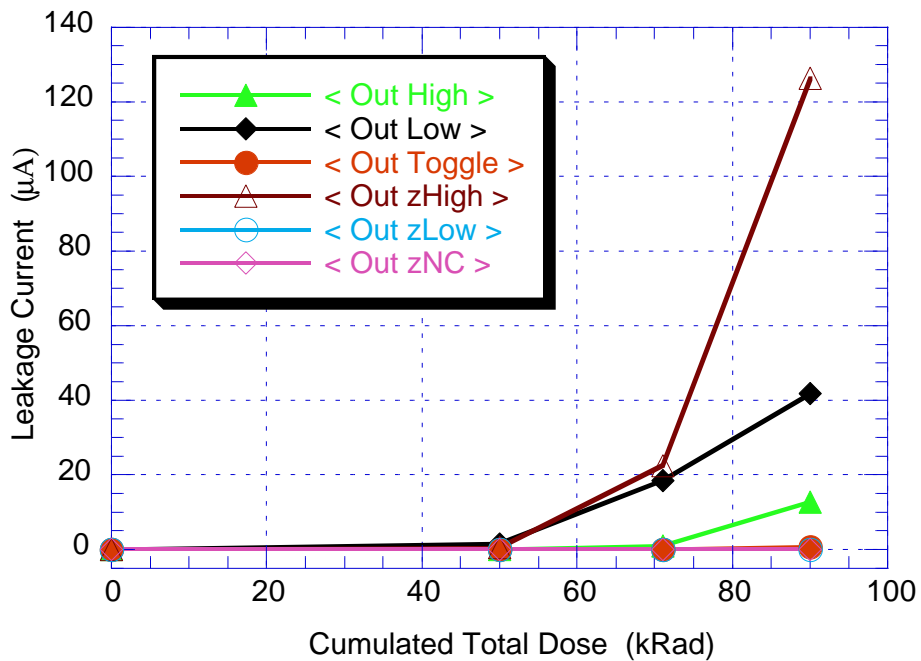

Fig. 6. Parameter measurements of output current high (I_{OZH}) for the 300 kHz dynamic operation mode at room temperature. The specification limit is ±10 µA. Data show both user outputs that have been static high, static low, toggled and tristated with external pull-up, pull-down and left floating during irradiation. Worst case is found to be pull-upped tristated outputs (Output zHigh).
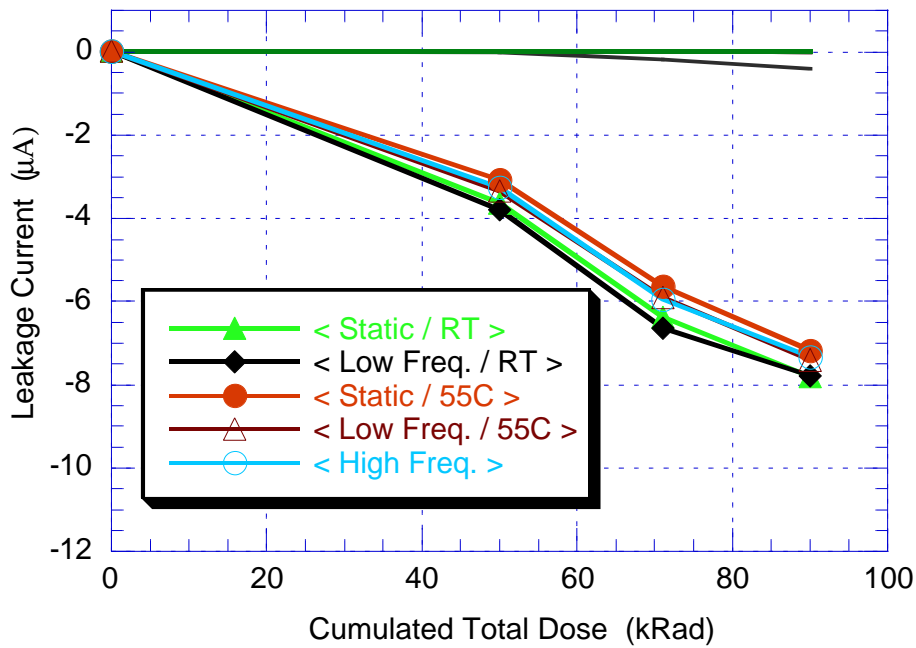
Fig. 7. Parameter measurements of Output Current Low (I_{OZL}) for the five test conditions. The specification limit is ±10 µA. Data with markers show outputs that have been static high during irradiation. Data without markers show all other outputs.
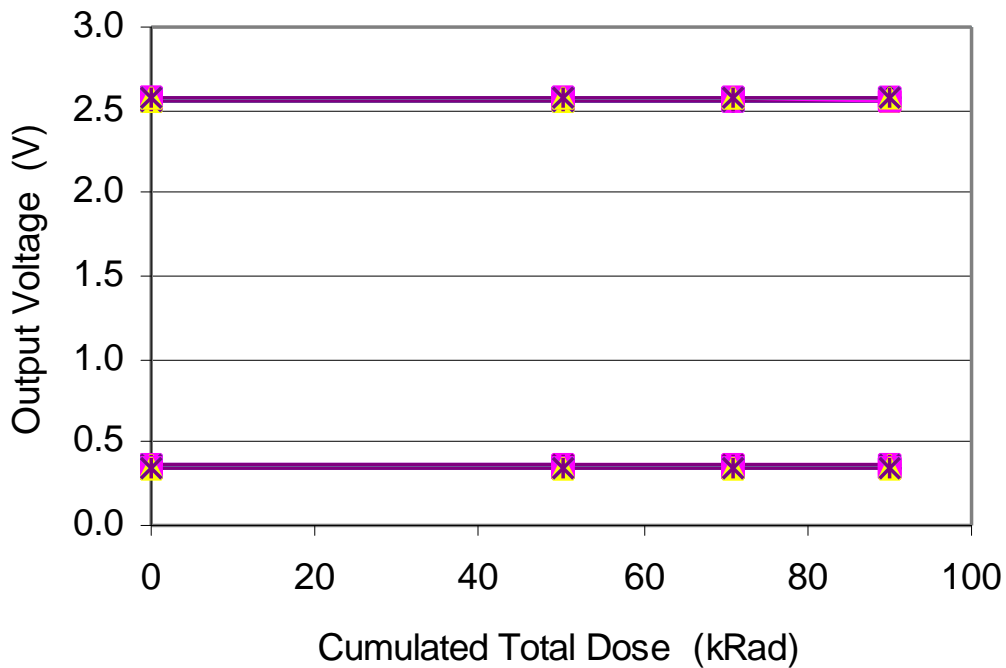

Fig. 8. Overview of all parameter measurements of Output Voltage Low and High (V_{OL}, V_{OH}) for the five test conditions. The specification limit is 0,5 V and 2,4 V respectively. All data is mean values of each type of state of the outputs during irradiation.

4.3   Propagation Delays of ^{60}Co-Irradiation

Measurements of propagation delays through binning circuits implemented in the design indicated very small damages with total dose, less than 3% increase. Static mode in room temperature (Static/RT) seems to be the worst case.

The pre irradiation time delays were about 100 ns. With a resolution of ±1ns for the test equipment, the resolution of the measurement is about ±1%.

This propagation delay consists not only of delays in internal logic but also of delays in the I/Os. This means that many different processes can give contribution to this measurement. In conclusion, the overall changes in time delays are very small for the internal logic.

Fig. 9. Propagation delay measurement: Positive pulse in, to positive pulse out, through binning circuits of buffers. Data show the change in time delay from initial value (~100 ns). Data from two binning circuits from all devices in all total dose test modes.

Fig. 10. Propagation delay measurement: Positive pulse in, to positive pulse out, through binning circuits of inverters. Data show the change in time delay from initial value (~118 ns). Data from two binning circuits from all devices in all total dose test modes.

Binning Circuit - Negative Pulse

Legend:
- Low Freq. / RT sn#01 Bin#01
- Low Freq. / RT sn#01 Bin#02
- Low Freq. / RT sn#02 Bin#01
- Low Freq. / RT sn#02 Bin#02
- Static / RT sn#03 Bin#01
- Static / RT sn#03 Bin#02
- Static / RT sn#04 Bin#01
- Static / RT sn#04 Bin#02
- Low Freq. / 55C sn#05 Bin#01
- Low Freq. / 55C sn#05 Bin#02
- Low Freq. / 55C sn#06 Bin#01
- Low Freq. / 55C sn#06 Bin#02
- Static / 55C sn#07 Bin#01
- Static / 55C sn#07 Bin#02
- Static / 55C sn#08 Bin#01
- Static / 55C sn#08 Bin#02
- High Freq. sn#09 Bin#01
- High Freq. sn#09 Bin#02
- High Freq. sn#10 Bin#01
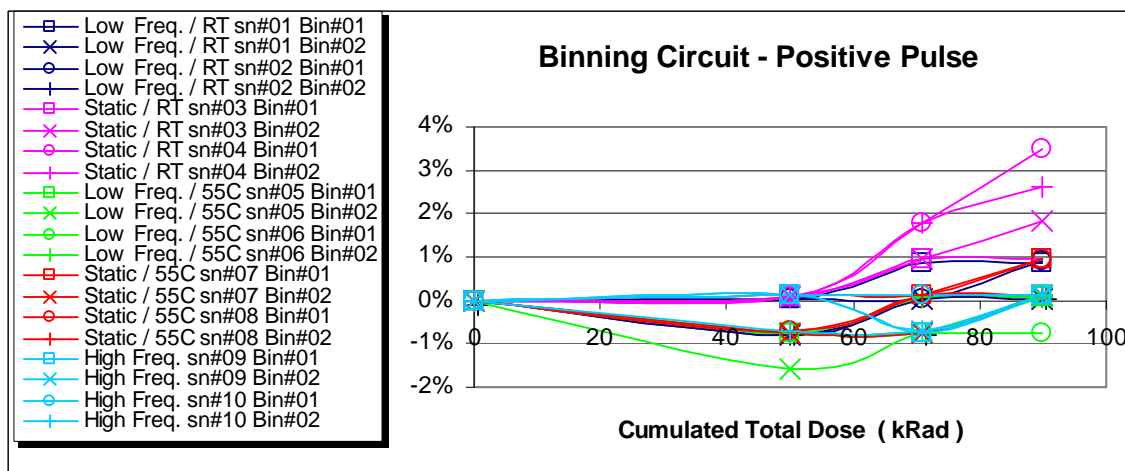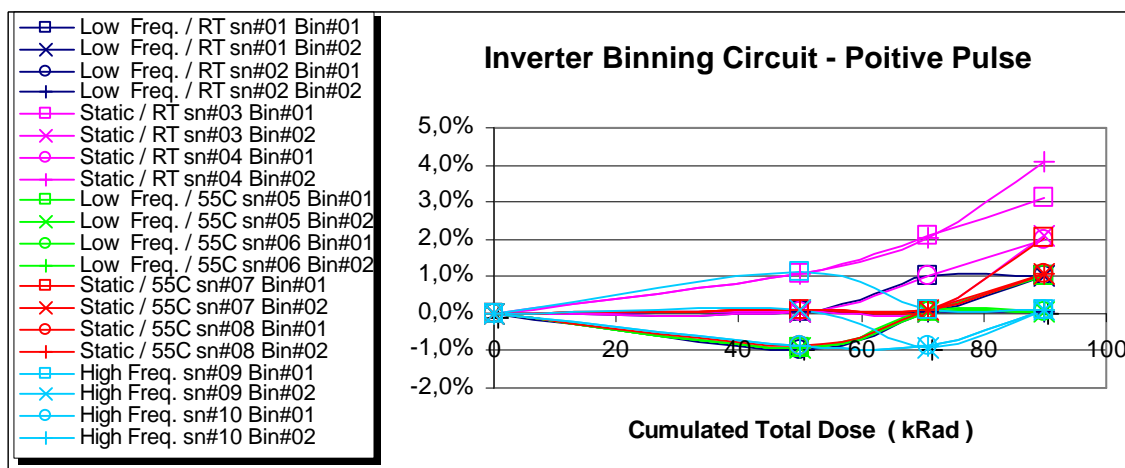- High Freq. sn#10 Bin#02

Cumulated Total Dose (kRad)

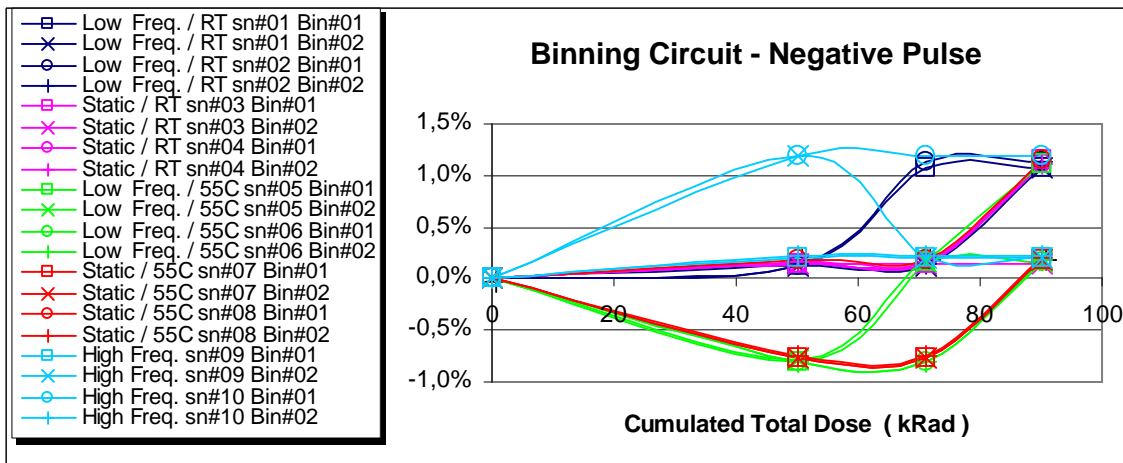Fig. 11. Propagation delay measurement: Negativ pulse in, to negative pulse out, through binning circuits of buffers. Data show the change in time delay from initial value (~105 ns). Data from two binning circuits from all devices in all total dose test modes.

Inverter Binning Circuit - Negative Pulse

Legend:
- Low Freq. / RT sn#01 Bin#01
- Low Freq. / RT sn#01 Bin#02
- Low Freq. / RT sn#02 Bin#01
- Low Freq. / RT sn#02 Bin#02
- Static / RT sn#03 Bin#01
- Static / RT sn#03 Bin#02
- Static / RT sn#04 Bin#01
- Static / RT sn#04 Bin#02
- Low Freq. / 55C sn#05 Bin#01
- Low Freq. / 55C sn#05 Bin#02
- Low Freq. / 55C sn#06 Bin#01
- Low Freq. / 55C sn#06 Bin#02
- Static / 55C sn#07 Bin#01
- Static / 55C sn#07 Bin#02
- Static / 55C sn#08 Bin#01
- Static / 55C sn#08 Bin#02
- High Freq. sn#09 Bin#01
- High Freq. sn#09 Bin#02
- High Freq. sn#10 Bin#01
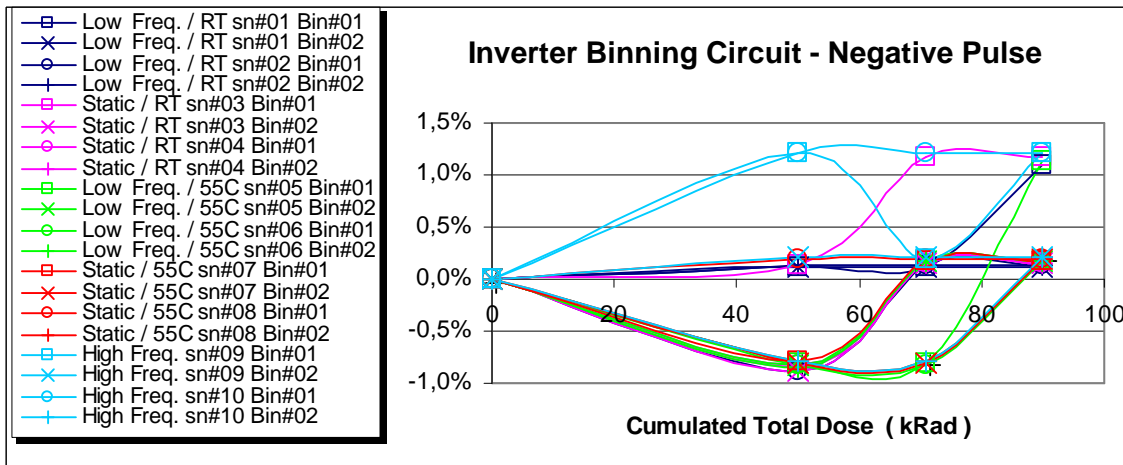- High Freq. sn#10 Bin#02

Cumulated Total Dose (kRad)

Fig. 12. Propagation delay measurement: Negativ pulse in, to negative pulse out, through binning circuits of inverters. Data show the change in time delay from initial value (~100 ns). Data from two binning circuits from all devices in all total dose test modes.

4.4   Proton Total Dose Results

Standby current as a function of cumulated total dose is shown in Fig.9 for the three operation conditions tested at room temperature. The overall behaviour is the same as for [60]Co. The increase in current starts, however, already at 40 kRad(Si). Considering the fact that these device type exhibit very fast annealing and the fact that the dose rates in the proton test were about 10 times higher, the increased leakage may be explained as a pure dose rate effect. The tested parts came from the same wafer lot as those from the ^{60}Co test.
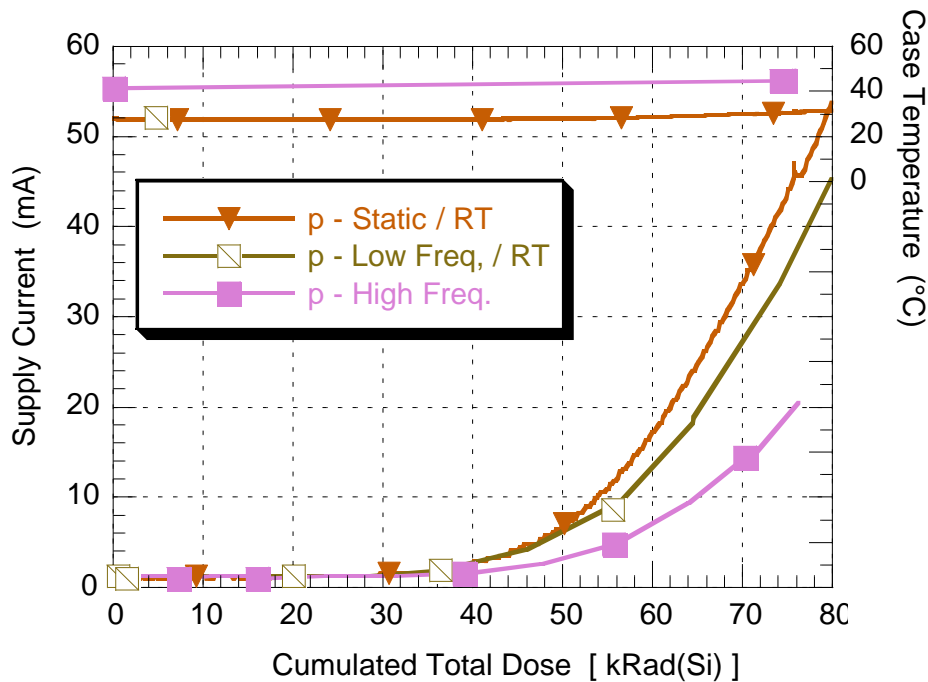

Fig. 13. Supply current as a function of proton total dose for the different test conditions. The upper part of the figure shows the case temperature for the three test conditions. The standby current behavior are very similar to those observed in the ^{60}Co tests, but with a faster increase in leakage current.

5.   CONCLUSION

Traditionally total dose testing is performed with static conditions during irradiation. This condition has been compared with more application like test conditions with higher temperature and dynamic operations. Total dose tests at 50°C show only small changes on the results, but by operating our device at 40MHz the measured total dose tolerance has been increased with 50%. Since our device had a chip temperature of 50°C at 40MHz operation, it could be concluded that the frequency has a major impact on the total dose results.
For a specific application where temperature and operation conditions is known it would be possible to increase the total dose level for the device by implement similar condition in the total dose testing. However, it is important to remember that by performing a more application like total dose test it is possible that some I/Os that mostly are static in the application will exhibit greater leakage damages than clocked I/O's will show in a dynamic test. It is recommended to perform parameter measurements on I/O's in all possible condition states.

The impact on total dose behaviour from protons indicates that the overall behaviour is the same as for ^{60}Co. The increase in current starts, however, already at 40 kRad(Si). Considering the fact that these device type exhibit very fast annealing and the fact that the dose rates in the proton test were about 10 times higher, the increased leakage may be explained as a pure dose rate effect.

6.   REFERENCES

[1]   S. Mattsson, F. Sturesson, M. Wiktorson, R. Harboe-Sørensen, *Influence of TID Test Condition on Actel A1425A,* ESA Radiation Report ESA_QCA991102T_C, January 2000.